Vacuum 199 (2022) 110971

Contents lists available at ScienceDirect

Vacuum

journal homepage: www.elsevier.com/locate/vacuum

An investigation into the mechanistic origin of thermal stability in thermal-microstructural-engineered additively manufactured Inconel 718

Michael Munther [a], Ali Tajyar [a], Noah Holtham [a], Lloyd Hackel [b], Ali Beheshti [c], Keivan Davami [a,*]

[a] Department of Mechanical Engineering, The University of Alabama, Tuscaloosa, AL, USA
[b] Curtiss Wright Surface Technologies, Metal Improvement Company, Livermore, CA, USA
[c] Department of Mechanical Engineering, George Mason University, Fairfax, VA, USA

ARTICLE INFO

Keywords:
Nickel-based superalloys
Laser peening
Microstructure engineering
Thermal stability

ABSTRACT

An obstacle hindering the applicability of surface modification techniques such as laser peening (LP) in high temperature systems stems from thermally-driven degradation of desirable, strain-induced material modifications. Illustrated in this work is a novel LP scheme termed laser peening plus thermal microstructure engineering (LP + TME) comprised of cyclic LP and the addition of intermittent 600 °C ($0.55T_m$) heat treatments designed to impart thermally-stable microstructural modifications in additively manufactured (AM) Inconel 718 (In718). Instrumented microindentation uncovered significant surface and sub-surface hardness enhancements exceeding 600 HV following LP + TME, a 20% increase over the as-built material. High magnitude compressive residual stresses exceeding −310 MPa were also measured following a 350-h 600 °C thermal exposure; a 25% increase compared to the material subjected to only a single laser shot. Thermal stabilization and overall material enhancement were determined to be the result of the formation of thermally-stable subgrains, subgrain and grain growth regulation through pinning effects, and dislocation-precipitate interactions.

1. Introduction

Mechanical surface modification techniques including laser peening (LP) have been successfully utilized to impart beneficial compressive residual stresses and work hardening in treated materials to mitigate surface-related modes of failure such as foreign object damage [1,2], stress corrosion cracking [3,4], and fatigue [5]. However, in sufficiently high temperature environments, favorable compressive residual stresses and crystalline defects relax and recover, lessening or reversing the effects of LP. Three primary mechanisms drive the thermal relaxation of residual stresses, which also contribute to minimizing work hardening effects through defect annihilation. In a scenario where operating temperatures are high enough to reduce the material's yield strength, the thermal activation of dislocations relieves elastic strains [6]. At lower temperatures (i.e. temperatures below yield strength decay), diffusional creep redistributes tensile and compressive residual stresses through material expansion or contraction [6]. Additionally, lower temperature exposure also enables stress relaxation through dislocation glide [6]. Ultimately, the ability to mitigate these mechanisms will expedite the effective use of LP in systems operating at temperature conducive to significant stress relaxation and defect recovery.

Recovery and relaxation mechanisms, specifically in In718 and in the context of laser peening, have been researched and identified to stem from the annihilation of meta-stable crystalline defects, stress relaxation, and the initial level of plastic strain [7–9]. Additional detrimental material evolutions at elevated temperatures such as grain growth, particle coarsening or dissolution, and material softening must also be dealt with when improving high temperature performance. Previous studies have understood and outlined the complications associated with the implementation of LP in high temperature environments [8,10–12]. Kattoura et al. uncovered a reduction in fatigue life resulting from the relaxation of LP-induced compressive residual stresses [11]. The evaluation of residual stress retention in multi-layered laser peening Inconel 718/718 Plus found that 65% of compressive residual stresses were retained after 120 h at 650 °C [13]. Furthermore, between 25% and 60% of initial compressive residual stresses following LP were preserved after one million fatigue cycles at 650 °C.

A few attempts have been made through the use of warm laser shock

* Corresponding author.
E-mail address: kdavami@eng.ua.edu (K. Davami).

https://doi.org/10.1016/j.vacuum.2022.110971
Received 31 December 2021; Received in revised form 3 February 2022; Accepted 22 February 2022
Available online 24 February 2022

peening (WLSP), or LP performed at elevated temperature on various materials, and found significant increases in fatigue life and surface hardness when compared to room temperature LP [14,15]. The observed enhancement in fatigue life and surface properties were reported to be the result of subgrain formation and increased dislocation pinning effects [16]. The WLSP technique is not applicable for industry at a large scale since the confinement media that can be used widely for complex geometries still need to be found. One could never consider it for a production application because there is not a practical way to implement it. An additional modified LP technique known as thermal engineering LP (TE-LP), which is the combination of a single warm LP and subsequent one-step heat treatment, was found to increase the pinning effect of precipitates [17]. With promising steps being taken to tackle the high temperature use of LP, it is the goal of the work to contribute to the advancement of this technology.

Herein, the mechanical properties and microstructure of Inconel 718 specimens processed with a novel technique called laser peening plus thermal microstructure engineering (LP + TME) which is comprised of cyclic treatments with sequential LP and annealing steps were studied (Experimental Methods in Supplementary Information). A significant increase in the stability of the microstructure and the residual stresses was observed. This higher stability was attributed to the modification of intermediate phase precipitation kinetics through repeated strain input, precipitate pinning effects, and complex interaction of precipitates and dislocations.

2. Results and discussion

2.1. Surface study

With material surface properties displaying sensitivity to various surface effects, i.e., residual stress, roughness, morphology, hardness, etc., surface-level investigations were carried out in target materials subject to one and four impact events, corresponding to the AM-LP and the AM-4LP-3HT/AM-4LP-3HT-E conditions, respectively. Illustrated in Fig. 1 are SEM micrographs and topographical profiles retrieved from the irradiated region of material subject to one and four impacts. A closer inspection of a centrally-located area within the irradiated surface reveals the presence of resolidified droplets which formed following material ablation in addition to several valley-like structures (Fig. 1b). Four impact events produced a markedly rougher surface with sharp, isolated peaks dispersed throughout the affected area (Fig. 1c). Further investigation utilizing stylus profilometry enabled the determination of the general spot topography produced through each treatment condition. An apparent surface relief was observed following a single impact (Fig. 1d), found to be approximately 1.2 mm wide, and 4 μm in depth, surrounded by material pileup situated at the spot perimeter, as depicted in Fig. 1d. A notably deeper, and wider relief structure was identified (Fig. 1e) as a result of four impacts with an estimated depth of 15 μm, and a width of 1.5 mm.

2.2. Microhardness and residual stress

Attaining a reasonable estimation of in-depth microhardness variation was done so through the indentation of a region adjacent to the treated surface with the indent scheme following the direction of the pressure wave (z-direction, Fig. 2a). Findings from this undertaking are provided in Fig. 2b, which illustrates the experimentally-determined Vickers microhardness and its evolution as a function of depth up to 2000 μm for each material. No noticeable variation in microhardness was observed in the as-built, untreated condition (AM), where values were seen to fluctuate between 500 HV and 510 HV. The absence of any

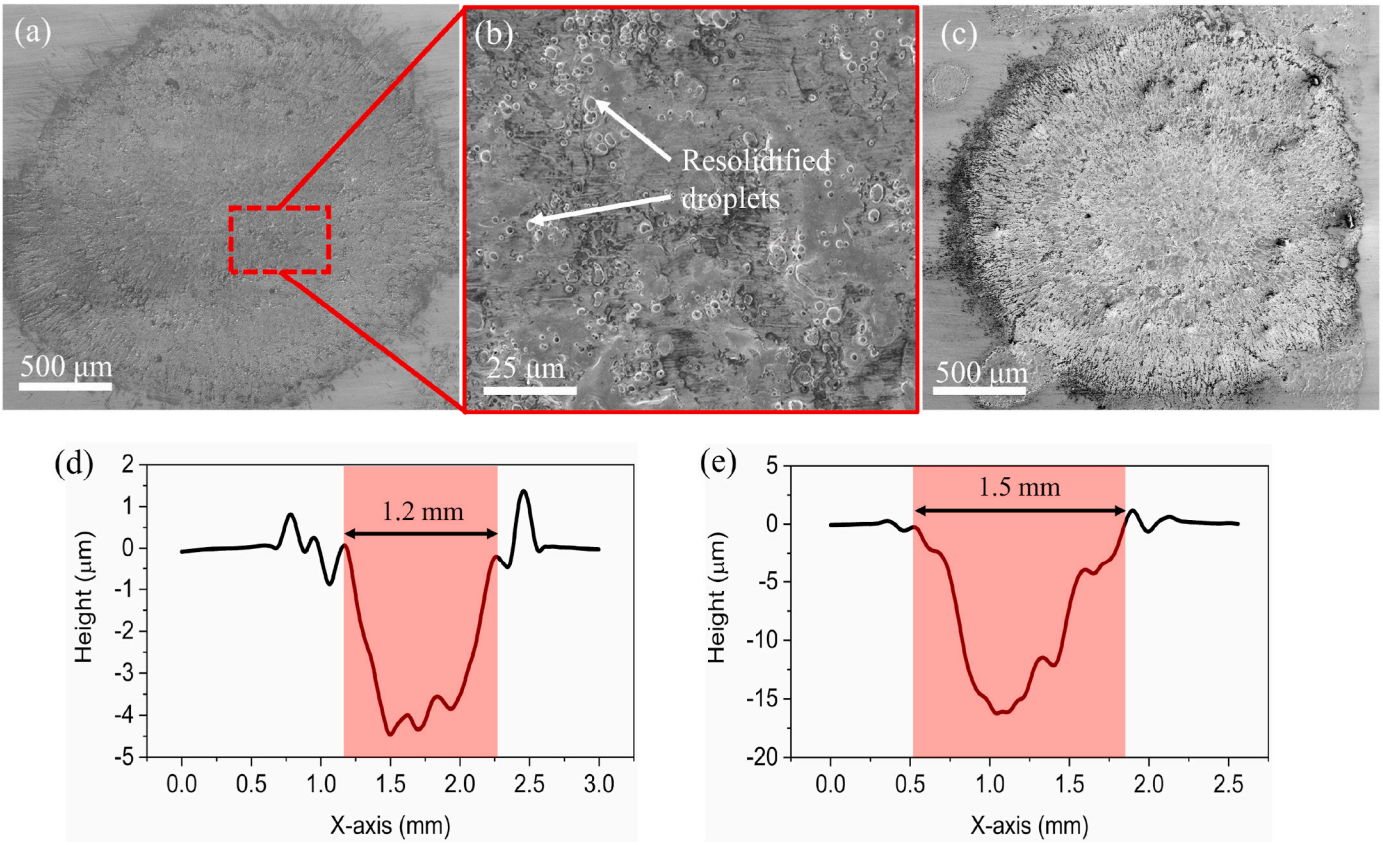

Fig. 1. SEM micrographs of (a) material surface following a single impact; (b) inset of irradiated region highlighting the presence of resolidified droplets and local variations in surface roughness; (c) material surface following four impacts; (d) topographical profile of impacted area after one shot; (e) topographical profile of impacted area after four shots.

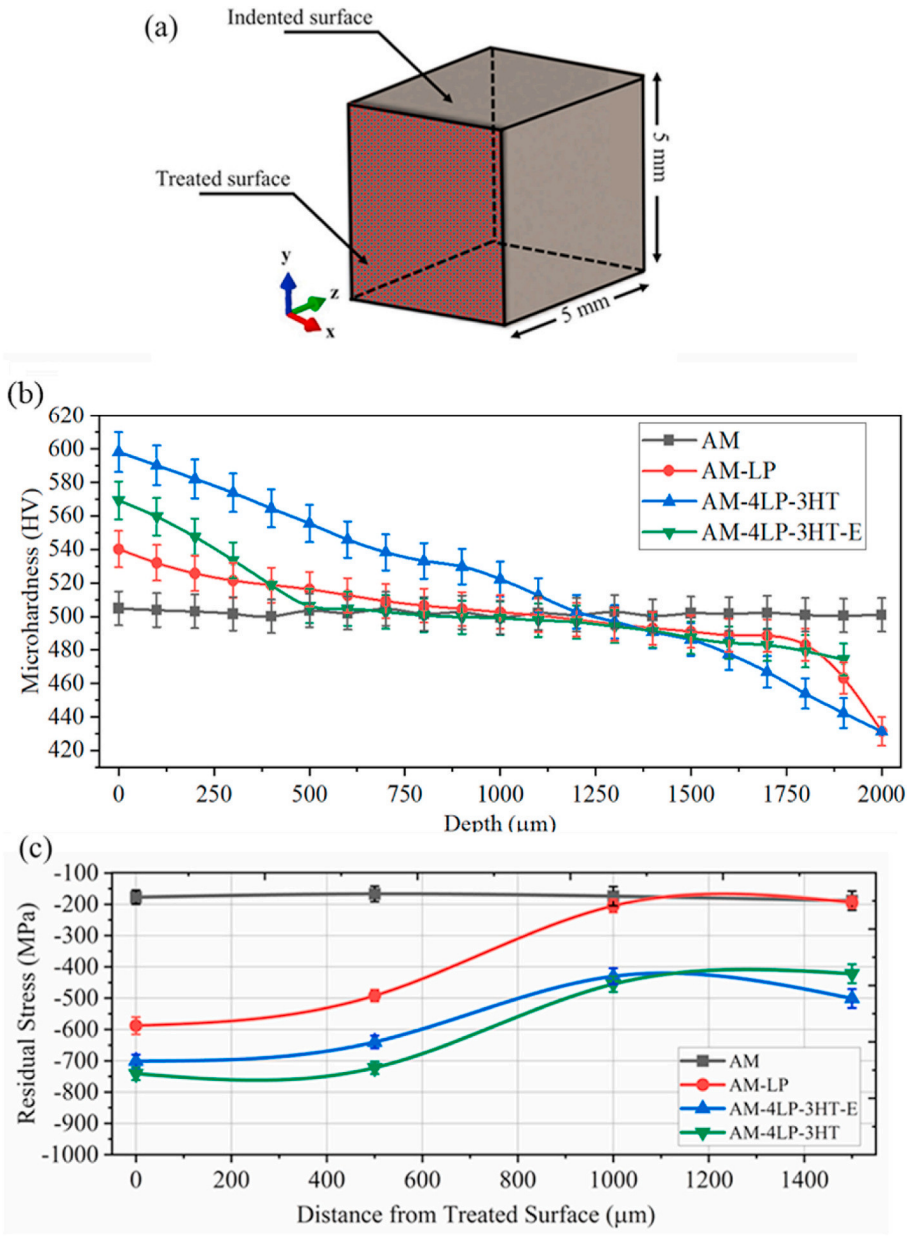

Fig. 2. (a) Schematic illustrating indented region with respect to treated surface; (b) microhardness distribution obtained from each material subject to each treatment condition; (c) residual stress distribution obtained from each material subject to each treatment condition.

apparent trend is unsurprising as the material was not subject to any surface modification or exposure to elevated temperature that would otherwise introduce discernible microhardness alterations. Following a single impact (AM-LP), a more apparent microhardness distribution was observed with highest microhardness intensification closest to the irradiated surface, where it monotonically decreased as a function of depth to approximately 750 μm. Here, microhardness was seen to increase by as much as 8% (540 HV) compared to the untreated condition. In this scenario, microhardness enhancement is the product of severe plastic deformation occurring as a result of the transfer of kinetic energy from the propagating pressure wave into the lattice where deformation occurs, enabling work hardening effects in the material.

With the combination of cyclic LP and the addition of intermittent thermal exposure (AM-4LP-3HT), substantial increases in microhardness were measured, with observed surface-level microhardness nearing 600 HV, 11% greater than what was seen following the single impact condition, and 18% greater than the untreated material. Additionally, the depth at which microhardness enhancements were realized appeared to extend 67% from 750 μm (AM-LP) to an estimated depth of 1250 μm. It is believed that the introduction of cyclic impact events enabled the activation of a larger quantity of slip systems, not only delivering an increase in overall defect density and therefore enhancing the material's hardening potential, but also driving preceding defect networks deeper into the material with each subsequent shock [18]. With LP + TME succeeded by a 350-h, 600 °C exposure (AM-4LP-3HT-E) a similar microhardness distribution was realized with the most significant enhancements accumulating at the immediate surface and eventually decreasing as a function of depth as the pressure wave loses energy to the material lattice. When compared to the pre-exposed condition (AM-4LP-3HT), there is an identifiable reduction in surface-level microhardness by as much as 5%, accompanied by a decrease in the hardened depth, with microhardness stabilization initiating 500 μm from the irradiated surface. Any level of reduction in both the magnitude and depth of microhardness enhancement was to be expected as the material was subject to temperatures greater than $0.5T_m$ for an extended duration. In this scenario, it is suspected that thermally-driven short

range diffusion occurred, wherein dense dislocation networks experienced moderate annihilation, lessening the likelihood of dislocation-dislocation interactions [19]. However, because defect annihilation occurs over a relatively short time frame (<1 h), it is suspected that there could be a number of microstructural avenues enabling the perceived 95% retention in surface-level microhardness, stemming from a potentially beneficial interaction between cyclic LP and intermittent thermal exposure [20].

Stress measurements through XRD were carried out in an effort to provide a reasonable estimation of the depth, magnitude, and thermal stability of compressive residual stresses prior to, and following thermal exposure. The experimentally determined residual stress distribution for each material is provided in Fig. 2c with stress reported as a function of distance from the treated surface. Reflecting similarities to the previously discussed microhardness findings, the identified residual stress state measured in the untreated (AM) material was determined to be compressive and stable (−175 MPa) throughout the measured region. The compressive nature of these stresses is thought to have originated during the build process; wherein localized heating produced a thermal expansion mismatch [21]. Furthermore, there is a possibility that crystallographic texture may be producing low-level micro-strain, influencing the observed residual stress state [22]. A single impact event produced notable increases in compressive residual stresses, with maximum surface-level stresses nearing −590 MPa, followed by stress stabilization occurring at an approximate depth of 1000 μm.

The presence of compressive residual stresses in this scenario is a product of both elastic and plastic material response to the pressure wave. Following the passage of the propagating pressure wave, a volume of strained material is compressed, where it then undergoes transverse expansion through the Poisson effect. Transverse expansion is resisted by the surrounding volume of untreated material which reacts elastically in response. Upon wave dissipation, the strained material acts to restrain the surrounding, contracting material where it is immobilized and gives way to the production of residual compressive stress [23]. Additionally, the presence of an identifiable stress gradient is a product of the continuous transfer of energy from the pressure wave into the material lattice as it propagates away from the irradiated surface [24]. The application of both cyclic LP and thermal exposure (AM-4LP-3HT) yielded a pronounced increase of the magnitude of surface-level stress by nearly 25% (−740 MPa) over the single-shot condition. In-depth stresses were also discovered to intensify, with stabilized stress values exceeding −450 MPa at a distance of 1000 μm from the treated surface. Following exposure to 600 °C for 350-h (AM-4LP-3HT-E), moderate stress relaxation was observed with surface-level stresses found to be −700 MPa – a 6% reduction compared to the pre-exposed AM-4LP-3HT condition. However, in-depth stresses were determined to be nearly identical to that of the pre-exposed condition, with a negligible difference in stress realized at 1000 μm.

2.3. Microstructural study

Elucidation of the measured variation in measured microhardness and residual stresses from a microstructural perspective was permitted through TEM investigations which uncovered a series of processes surmised to drive not only appreciable material improvement, but thermal stabilization at temperatures exceeding $0.5T_m$. Featured in Fig. 3 are TEM micrographs of the surface and immediate substructure of the In718 specimens wherein notable microstructural features were detected. In Fig. 3a, which depicts the topmost 1500 nm of as-built (AM) In718, no discernible transformative structures were located aside from a distribution of acicular δ-phases (Ni_3Nb). Here, the solution of nonequilibrium δ originated through Nb segregation occurring during the DMLS process [25]. Alternatively, the presence of fine subgrain highlighted in Fig. 3b appeared to dominate the microstructural changes occurring in the uppermost plastically deformed region of the AM-LP material to a depth of about 200 nm. Here, subgrains were measured to be 60 nm–80 nm in length, with elongated ellipsoid morphologies. Large subgrain networks comprised of smaller, equiaxed 30 nm–50 nm subgrain extending 600 nm from the surface were visualized in AM-4LP-3HT-E (Fig. 3c). Upon further inspection, deeper subgrain

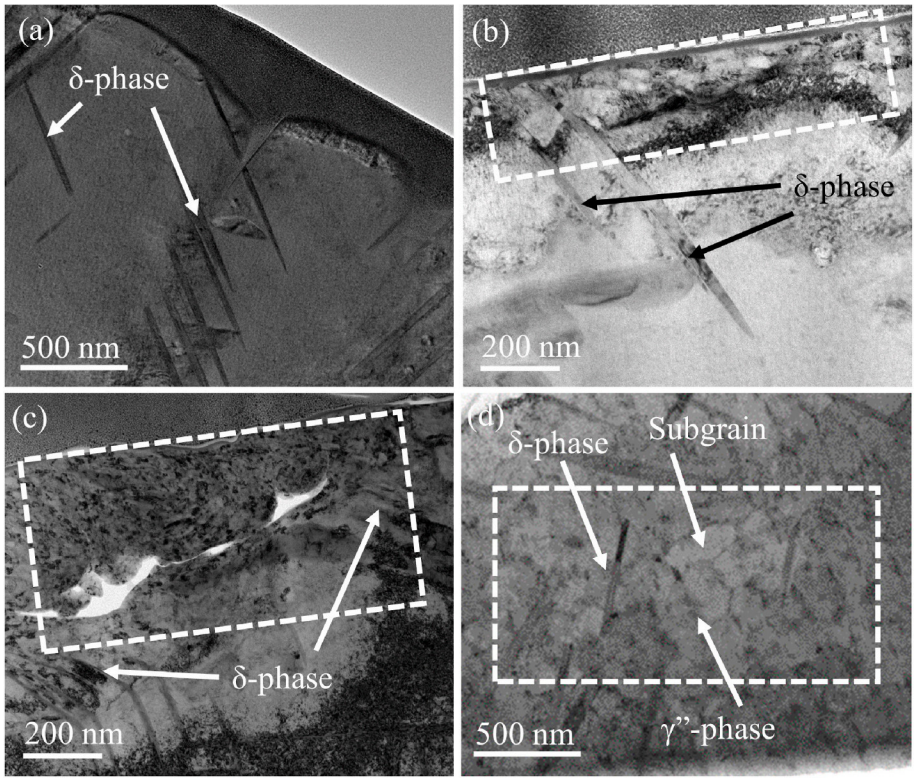

Fig. 3. TEM micrograph of (a) the surface and near-surface region of as-built (AM) material highlighting the lack of any mechanisms responsible for property modification; (b) the presence of subgrains (white box) and δ-phases in the top 200 nm of the AM-LP sample; (c) presence of subgrains (white box) and δ-phases in the top 500 nm of the AM-4LP-3HT-E sample; and (d) larger subgrains located approximately 1000 nm from the treated surface (white box) as well as dispersed δ-phases in AM-4LP-3HT-E.

networks located approximately 1000 nm from the surface comprised of larger, 200 nm–300 nm subgrain were observed in AM-4LP-3HT-E (Fig. 3d, as highlighted by the white box), a consequence of cyclic plasticity, driving dislocation networks deeper into the material. From a microstructural point of view, the presence of subgrain observed at appreciable depth presents barriers to dislocation mobility, restricting their motion to the material surface [11].

Subgrain formation, a consequence of plastic deformation, has been known to occur as a result of laser peening. This involves the development of intragranular dislocation lines and the pileup of dislocation lines leading to the formation of dislocation tangles. With the buildup of dislocations and the addition of thermal input, the defect structure begins to organize into subgrains [26]. The total dislocation density during deformation increases (i.e. during cyclic LP), which is concurrent with increased work hardening due to long range stresses acting on dislocations [27]. Dislocations in the presence of long range stresses and heat input will tend to reorganize into low energy configurations, or subgrains. The overall process of subgrain formation following laser and heat treatment is known to be stable at elevated temperature and has good resistance to recrystallization [28,29]. While the reorganization of meta-stable defects involves minimal levels of stress relaxation, the degree of stress relaxation associated with subgrain formation is not enough to significantly impact dislocation density [30]. The benefit of this mechanism lies in the retention of favorable defect structures which influence not only surface microhardness but may aid in preserving compressive residual stresses beyond typical relaxation temperatures.

While the formation of subgrains has been identified to contribute to microhardness and residual stress retention, other mechanisms which aid to stabilize subgrains and provide further strength enhancement were observed in the microstructures of the treated material. The presence of precipitated phases, specifically δ and γ'', are believed to interact favorably with LP-induced microstructures through subgrain boundary and defect pinning effects. Fig. 3b–d illustrate dispersed δ-phases within subgrain networks where during deformation, δ-phases pin glide bands generated during deformation, impeding the slipping of dislocations [31]. The identity of the δ phases were verified via selected area electron diffraction (SAED) patterns (see Supplementary Information, Fig. S5). Additionally, γ" precipitating along defect sites, as illustrated in Fig. 3d, is also thought to contribute to the stability by preventing subgrain coarsening at elevated temperatures [32].

Furthermore, hard δ-phases, while effective barriers to dislocation motion, are integral to regulating grain coarsening mechanisms associated with thermal input [33,34]. Fig. 4 (a,b) highlights two examples of the preferential nucleation of δ-phases along grain boundaries in AM-4LP-3HT-E. Here, the intergranular boundaries are decorated with δ-phases with the addition of intragranular δ. As the properties of In718 are particularly sensitive to microstructure, especially grain size, stable δ-phases prevents grain growth during high temperature deformation [35]. Additional TEM images are presented in the Supplementary Information.

Another possible strengthening effect of LP + TME might be attributed to the activation of Orowan and Friedel mechanisms. These mechanisms have been discussed extensively in our previous work [36,37]. Cyclic LP process and the induced strain along with the heat treatment steps facilitate the early precipitation of the strengthening phases. The interaction between the dislocations and precipitates results in the stabilization and strengthening of the specimens treated with the LP + TME method. Depending on the particle size, these interactions might be categorized as Friedel cutting or Orowan bypassing mechanism. When the strengthening precipitates have a small size, moving dislocations shear through them. This is not the case however for bigger particles as in that case shearing requires more energy. When mobile

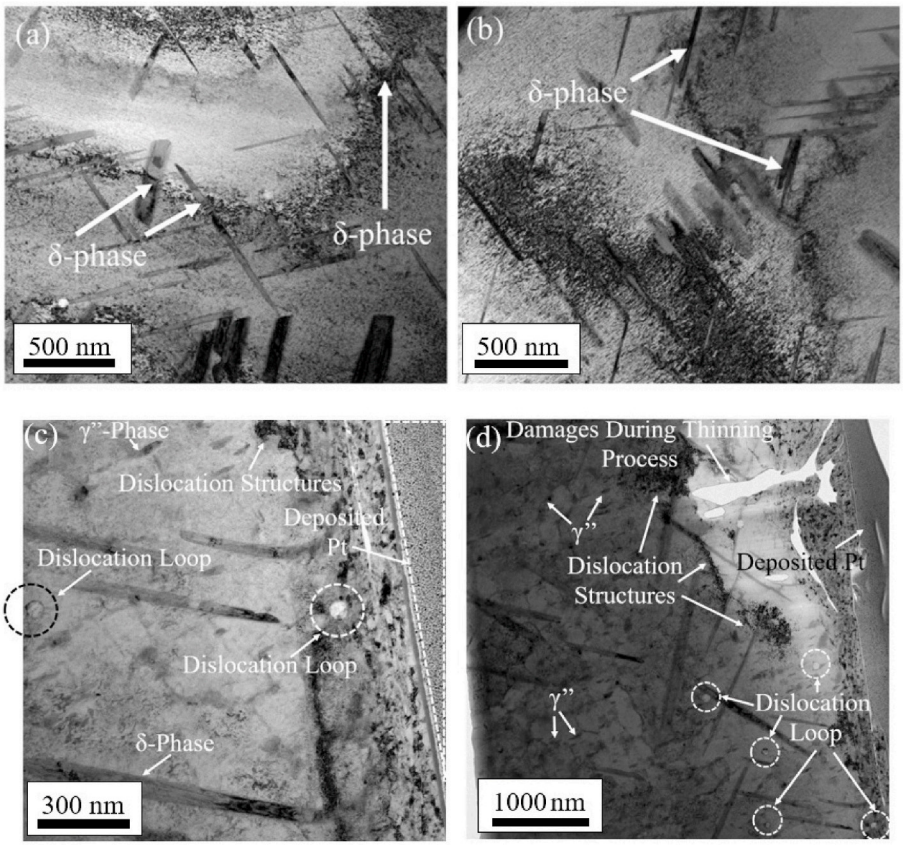

Fig. 4. (a) and (b) TEM micrographs illustrating the preferential nucleation of δ-phases on grain boundaries in AM-4LP-3HT-E, (c) and (d) dislocation loops identified in AM-4LP-3HT-E right beneath the treated surface.

dislocations meet larger strengthening precipitates, they bow around the precipitates through Orowan looping (Fig. 4 (c, d)). The loop formation leads to a reduction in the particle spacing, therefore, a higher bypassing stress is needed to force the movement of additional dislocations.

3. Conclusion

Additively manufactured Inconel 718 treated with the novel, LP + TME process exhibited a 95% retention in measured surface hardness after exposure to 600 °C for 350 h. TEM investigations of treated material uncovered an array of mechanisms owing to appreciable material enhancement and thermal stability. It was found that the reorganization of dislocations into subgrains, and the precipitation of intermediate phases, namely δ and γ'' interacted favorably to provide material strength and microstructural stability. It can therefore be determined that the combination of both strain and thermal input provides a synergistic effect in producing and preserving beneficial microstructure evolution which would otherwise be impossible without the addition of intermittent heat treatment.

CRediT authorship contribution statement

Michael Munther: Writing – original draft, Investigation, Formal analysis. **Ali Tajyar:** Writing – original draft, Formal analysis. **Noah Holtham:** Formal analysis. **Lloyd Hackel:** Formal analysis. **Ali Beheshti:** Writing – original draft, Formal analysis. **Keivan Davami:** Writing – original draft, Writing – review & editing, Funding acquisition, Supervision.

Declaration of competing interest

The authors declare that they have no known competing financial interests or personal relationships that could have appeared to influence the work reported in this paper.

Acknowledgements

The authors would like to acknowledge the Alabama Transportation Institute for the continual support of the researchers responsible for authoring this work. The project has also received additional support from the National Science Foundation, CMMI, Advanced Manufacturing Program (award number: 2029059).

Appendix A. Supplementary data

Supplementary data to this article can be found online at https://doi.org/10.1016/j.vacuum.2022.110971.

References

[1] S. Zabeen, M. Preuss, P.J. Withers, Evolution of a laser shock peened residual stress field locally with foreign object damage and subsequent fatigue crack growth, Acta Mater. 83 (2015) 216–226, https://doi.org/10.1016/j.actamat.2014.09.032.
[2] B. Lin, C. Lupton, S. Spanrad, J. Schofield, J. Tong, Fatigue crack growth in laser-shock-peened Ti-6Al-4V aerofoil specimens due to foreign object damage, Int. J. Fatig. 59 (2014) 23–33, https://doi.org/10.1016/j.ijfatigue.2013.10.001.
[3] J.Z. Lu, K.Y. Luo, D.K. Yang, X.N. Cheng, J.L. Hu, F.Z. Dai, H. Qi, L. Zhang, J. S. Zhong, Q.W. Wang, Y.K. Zhang, Effects of laser peening on stress corrosion cracking (SCC) of ANSI 304 austenitic stainless steel, Corrosion Sci. 60 (2012) 145–152, https://doi.org/10.1016/j.corsci.2012.03.044.
[4] O. Hatamleh, P.M. Singh, H. Garmestani, Stress corrosion cracking behavior of peened friction stir welded 2195 aluminum alloy joints, J. Mater. Eng. Perform. 18 (2009) 406–413, https://doi.org/10.1007/s11665-008-9303-8.
[5] O. Hatamleh, J. Lyons, R. Forman, Laser and shot peening effects on fatigue crack growth in friction stir welded 7075-T7351 aluminum alloy joints, Int. J. Fatig. 29 (2007) 421–434, https://doi.org/10.1016/J.IJFATIGUE.2006.05.007.
[6] M.R. James, Relaxation of Residual Stresses an Overview, vol. 4, Pergamon Press, 1987, pp. 349–365. Advances in Surface Treatments. Technology–Applications–Effects.
[7] N. Masmoudi, L. Castex, A. Bertoli, Influence of temperature and time on the stress relaxation process of shot peened IN 100 superalloys, Matériaux Tech. 77 (1989) 29–36.
[8] A. Telang, A.S. Gill, S.R. Mannava, D. Qian, V.K. Vasudevan, Effect of temperature on microstructure and residual stresses induced by surface treatments in Inconel 718 SPF, Surf. Coating. Technol. 344 (2018) 93–101, https://doi.org/10.1016/j.surfcoat.2018.02.094.
[9] M. Kattoura, S.R. Mannava, D. Qian, V.K. Vasudevan, Effect of laser shock peening on residual stress, microstructure and fatigue behavior of ATI 718Plus alloy, Int. J. Fatig. 102 (2017) 121–134, https://doi.org/10.1016/j.ijfatigue.2017.04.016.
[10] Z.P. Tong, X.D. Ren, W.F. Zhou, S. Adu-Gyamfi, L. Chen, Y.X. Ye, Y.P. Ren, F.Z. Dai, J.D. Yang, L. Li, Effect of laser shock peening on wear behaviors of TC11 alloy at elevated temperature, Opt Laser. Technol. 109 (2019) 139–148, https://doi.org/10.1016/J.OPTLASTEC.2018.07.070.
[11] M. Kattoura, S.R. Mannava, D. Qian, V.K. Vasudevan, Effect of laser shock peening on elevated temperature residual stress, microstructure and fatigue behavior of ATI 718Plus alloy, Int. J. Fatig. 104 (2017) 366–378, https://doi.org/10.1016/J.IJFATIGUE.2017.08.006.
[12] Y. Li, L. Zhou, W. He, G. He, X. Wang, X. Nie, B. Wang, S. Luo, Y. Li, The strengthening mechanism of a nickel-based alloy after laser shock processing at high temperatures, Sci. Technol. Adv. Mater. 14 (2013), 055010, https://doi.org/10.1088/1468-6996/14/5/055010.
[13] M. Kattoura, S.R. Mannava, D. Qian, V.K. Vasudevan, Effect of laser shock peening on elevated temperature residual stress, microstructure and fatigue behavior of ATI 718Plus alloy, Int. J. Fatig. 104 (2017) 366–378, https://doi.org/10.1016/j.ijfatigue.2017.08.006.
[14] C. Ye, Y. Liao, G.J. Cheng, Warm laser shock peening driven nanostructures and their effects on fatigue performance in aluminium alloy 6160, Adv. Eng. Mater. 12 (2010), https://doi.org/10.1002/adem.200900290. NA-NA.
[15] J.Z. Zhou, X.K. Meng, S. Huang, J. Sheng, J.Z. Lu, Z.R. Yang, C. Su, Effects of warm laser peening at elevated temperature on the low-cycle fatigue behavior of Ti6Al4V alloy, Mater. Sci. Eng., A 643 (2015) 86–95, https://doi.org/10.1016/J.MSEA.2015.07.017.
[16] Y. Liao, C. Ye, G.J. Cheng, [INVITED] A review: warm laser shock peening and related laser processing technique, Opt Laser. Technol. 78 (2016) 15–24, https://doi.org/10.1016/J.OPTLASTEC.2015.09.014.
[17] Y. Liao, G.J. Cheng, Controlled precipitation by thermal engineered laser shock peening and its effect on dislocation pinning: multiscale dislocation dynamics simulation and experiments, Acta Mater. 61 (2013) 1957–1967, https://doi.org/10.1016/J.ACTAMAT.2012.12.016.
[18] R. Bikdeloo, G.H. Farrahi, A. Mehmanparast, S.M. Mahdavi, Multiple laser shock peening effects on residual stress distribution and fatigue crack growth behaviour of 316L stainless steel, Theor. Appl. Fract. Mech. 105 (2020) 102429, https://doi.org/10.1016/j.tafmec.2019.102429.
[19] W. Cao, M. Khadhraoui, B. Brenier, J.Y. Guédou, L. Castex, Thermomechanical relaxation of residual stress in shot peened nickel base superalloy, Mater. Sci. Technol. 10 (1994) 947–954, https://doi.org/10.1179/mst.1994.10.11.947.
[20] P.S. Prevey, The Effect of Cold Work on the Thermal Stability of Residual Compression in Surface Enhanced IN718, 2000.
[21] D.W. Brown, J.D. Bernardin, J.S. Carpenter, B. Clausen, D. Spernjak, J. M. Thompson, Neutron diffraction measurements of residual stress in additively manufactured stainless steel, Mater. Sci. Eng. 678 (2016) 291–298, https://doi.org/10.1016/j.msea.2016.09.086.
[22] L.M. Sochalski-Kolbus, E.A. Payzant, P.A. Cornwell, T.R. Watkins, S.S. Babu, R. R. Dehoff, M. Lorenz, O. Ovchinnikova, C. Duty, Comparison of residual stresses in Inconel 718 simple parts made by electron beam melting and direct laser metal sintering, Metall. Mater. Trans.: Physical Metallurgy and Materials Science 46 (2015) 1419–1432, https://doi.org/10.1007/s11661-014-2722-2.
[23] H. Tanaka, K. Akita, Y. Sano, S. Ohya, Compressive residual stress generation process by laser peening without pre-coating, Transactions on The Built Environment 85 (2006) 1743–3509, https://doi.org/10.2495/HPSM06035.
[24] P. Peyre, R. Fabbro, P. Merrien, H.P. Lieurade, Laser shock processing of aluminium alloys. Application to high cycle fatigue behaviour, Mater. Sci. Eng. 210 (1996) 102–113, https://doi.org/10.1016/0921-5093(95)10084-9.
[25] K.T. Son, M.E. Kassner, K.A. Lee, The creep behavior of additively manufactured Inconel 625, Adv. Eng. Mater. 22 (2020) 1900543, https://doi.org/10.1002/adem.201900543.
[26] J.Z. Zhou, S. Huang, J. Sheng, J.Z. Lu, C.D. Wang, K.M. Chen, H.Y. Ruan, H. S. Chen, Effect of repeated impacts on mechanical properties and fatigue fracture morphologies of 6061-T6 aluminum subject to laser peening, Mater. Sci. Eng. 539 (2012) 360–368, https://doi.org/10.1016/j.msea.2012.01.125.
[27] K.Linga Murty, Materials' Ageing and Degradation in Light Water Reactors : Mechanisms and Management, Woodhead Publishing, 2013.
[28] A. Bhaduri, Mechanical Properties and Working of Metals and Alloys, Springer, 2019.
[29] R.A. Perkins, The effect of thermal-mechanical treatments on the structure and properties of refractory metals, in: Refractory Metal Alloys Metallurgy and Technology, Springer US, 1968, pp. 85–120, https://doi.org/10.1007/978-1-4684-9120-3_3.
[30] R. Wawszczak, A. Baczmański, M. Marciszko, M. Wróbel, T. Czeppe, K. Sztwiertnia, C. Braham, K. Berent, Evolution of microstructure and residual stress during annealing of austenitic and ferritic steels, Mater. Char. 112 (2016) 238–251, https://doi.org/10.1016/j.matchar.2015.12.019.
[31] S.H. Zhang, H.Y. Zhang, M. Cheng, Tensile deformation and fracture characteristics of delta-processed Inconel 718 alloy at elevated temperature, Mater. Sci. Eng. 528 (2011) 6253–6258, https://doi.org/10.1016/j.msea.2011.04.074.

[32] M.C. Somani, K. Muraleedharan, N.C. Birla, V. Singh, Y.V.R.K. Prasad, Hot deformation characteristics of INCONEL alloy MA 754 and development of a processing map, Metall. Mater. Trans. 25 (1994) 1693–1702, https://doi.org/10.1007/BF02668534.

[33] S. Chenna Krishna, G.S. Rao, S.K. Singh, S.V.S. Narayana Murty, G. Venkatanarayana, A.K. Jha, B. Pant, P.V. Venkitakrishnan, Processing and characterization of sub-delta solvus forged hemispherical forgings of Inconel 718, J. Mater. Eng. Perform. 25 (2016) 5477–5485, https://doi.org/10.1007/s11665-016-2377-9.

[34] P. Nandwana, M. Kirka, A. Okello, R. Dehoff, Electron beam melting of Inconel 718: effects of processing and post-processing, Mater. Sci. Technol. 34 (2018) 612–619, https://doi.org/10.1080/02670836.2018.1424379.

[35] P.J.P. Kañetas, L.A.R. Osorio, M.P.G. Mata, M.D. La Garza, V.P. López, Influence of the delta phase in the microstructure of the Inconel 718 subjected to "delta-processing" heat treatment and hot deformed, Procedia Materials Science 8 (2015) 1160–1165, https://doi.org/10.1016/j.mspro.2015.04.180.

[36] M. Munther, R. Rowe, M. Sharma, L. Hackel, K. Davami, Thermal stabilization of additively manufactured superalloys through defect engineering and precipitate interactions, Mater. Sci. Eng., A 798 (2020) 140119.

[37] M. Munther, T. Martin, A. Tajyar, L. Hackel, A. Beheshti, K. Davami, Laser shock peening and its effects on microstructure and properties of additively manufactured metal alloys: a review, Engineering Research Express 2 (2020), 022001.